16 February 2001

ELSEVIER

Chemical Physics Letters 335 (2001) 111–122

CHEMICAL PHYSICS LETTERS

www.elsevier.nl/locate/cplett

Towards selective recoupling and mutual decoupling of dipolar-coupled spin pairs in double-quantum magic-angle spinning NMR experiments on multiply labelled solid-state samples

Ingo Schnell *, Anthony Watts

Biomembrane Structure Unit, Biochemistry Department, University of Oxford, South Parks Road, Oxford OX1 3QU, UK

Received 6 September 2000; in final form 7 December 2000

Abstract

In solid-state magic-angle spinning NMR experiments, the combination of selective inversion and dipolar recoupling schemes, such as DANTE and C7, allows double-quantum coherences to be selectively generated between distinct types of spins, as is experimentally demonstrated here. In such selective inversion and multiple quantum excitation experiments, the double quantum coherences are excited between spins with identical polarisation, but not between spins with opposite polarisation. By investigating the decay of longitudinal magnetisation or the build-up of double-quantum coherences, the respective dipolar pair couplings can be individually measured in the presence of perturbing couplings, which may even significantly exceed the coupling of interest.

1. Introduction

A major concern of modern solid-state NMR experiments is the determination of molecular structure through the use of dipolar couplings. While magic-angle spinning (MAS) and radio-frequency (RF) heteronuclear decoupling techniques are essential for the enhancement of spectral resolution, a variety of dipolar recoupling techniques [1–11] have been developed in order to exploit the distance and orientational information inherent in dipolar couplings between pairs of nuclei. In particular, a number of approaches have been designed which employ dipolar recoupling for the excitation of multiple-quantum (MQ) coherences among dipolar coupled spin-1/2 nuclei and allow the investigation of local molecular structure through the determination of internuclear distances [12–17] and molecular torsional angles [18–23]. For the nuclei of interest, the dipolar couplings between them need to be selectively observed while perturbing interactions, as well as background signals, are to be separated or suppressed. In many cases, this selectivity is achieved by chemically or biochemically introducing a specific isotopic labelling scheme. Alternatively or additionally, the NMR experiments provide, to a certain extent, selective information by spectrally resolving the chemical shifts. However, the observation of weak dipolar couplings in

* Corresponding author. Present address: Max-Planck-Institut für Polymerforschung, Postfach 3148, D-55021 Mainz, Germany. Fax: +49 6131 379 100.

E-mail address: schnelli@mpip-mainz.mpg.de (I. Schnell).

0009-2614/01/$ - see front matter
PII: S0009-2614(01)00027-6

the presence of strong perturbing couplings represents a serious problem for the investigation of multiple-spin systems in NMR. Hence, to facilitate work with multiply labelled samples and to gain simultaneous access to structural parameters, it is desirable to improve the selection techniques available to dipolar MQ MAS NMR experiments.

A well established technique utilising the chemical shift separation of resonance lines for selective dipolar recoupling is rotational resonance (RR) [24,25], which has been used for internuclear distance determinations [12–17] as well as for selective excitation of double-quantum (DQ) coherences [26,27]. The RR approach is based on the observation that, under MAS, the dipolar interaction between two spins i and j is recoupled if the chemical shift difference $\Delta\omega_{CS} = \omega_{CS}^{(i)} - \omega_{CS}^{(j)}$ is a small integer multiple of the MAS frequency ω_R, i.e., $\Delta\omega_{CS} = n\omega_R$. Experimentally, the $n = 1$ condition is commonly applied. Despite the unquestionable usefulness of RR, the latter condition imposes a serious restriction on the experiments, because the MAS frequency is determined by the chemical shift difference of the nuclei of interest, and cannot accommodate further the needs of homo- and heteronuclear dipolar decoupling, sideband suppression, and sample geometry. Moreover, the resonance condition is relatively sensitive, such that even small distributions of chemical shifts lead to less efficient recoupling performance. An experimental approach overcoming the latter problem has recently been proposed [28].

In this context, an alternative selection technique allowing more flexibility on the MAS frequency, or on the chemical shift difference, would be helpful. Here, we present an approach employing broadband dipolar recoupling pulse-sequences, which can be tailored for DQ excitation while compensating for chemical shift differences, frequency offsets and other perturbing interactions, as demonstrated extensively for helical pulse sequences [5,7,10]. In contrast to RR, which recouples the dipolar interaction only between two distinct types of spins, the selectivity is achieved by preparing an initial state of longitudinal magnetisation (LM), in which spins are selectively inverted before the recoupling pulse sequence is applied. For simplicity, this approach will henceforth be referred to as selective inversion and MQ excitation (SIMQEX). In addition, we discuss alternative versions for performing DQ-filtered experiments, following either the decay of LM, or the build-up of DQ coherences. For spin pairs, the curves theoretically contain the same information about the underlying coupling and are mirror images of each other, but experimentally differences in the relaxation behaviour are observed.

2. Theory

The effect of dipolar recoupling pulse sequences applicable for the excitation of DQ coherences under MAS conditions can, in general, be described by an average Hamiltonian of the form:

$$\boldsymbol{H}_{DQ} = \sum_{i<j} \omega_D^{(ij)} \left(\boldsymbol{T}_{2,+2}^{(ij)} + \boldsymbol{T}_{2,-2}^{(ij)} \right), \tag{1}$$

where the sum includes all pairs of spins i and j, $\boldsymbol{T}_{2,\pm2}^{(ij)}$ represents the second-order component of a second-rank spherical tensor operator, and $\omega_D^{(ij)}$ is a numerical factor which depends on the pulse sequence. In general, the latter factor contains the dipolar coupling D_{ij} between the spins i and j, which is given by $D_{ij} = -\mu_0/4\pi\hbar\gamma_i\gamma_j/r_{ij}^3$ (in rad s^{-1}), where γ_i and γ_j denote the magnetogyric ratios, and r_{ij} is the internuclear distance. In the case of the C7 sequence [5], the norm of the numerical factor is

$$\omega_D^{(ij)} = -\frac{343\sqrt{1+\sin\pi/14}}{520\pi\sqrt{2}} \sin 2\beta_{ij} D_{ij},$$

where β_{ij} and γ_{ij} denote the azimuthal and polar angle of the internuclear vector $\boldsymbol{r}_{ij}$, respectively. Our considerations are restricted to the magnitude of the factor, while disregarding its phase, because the following discussion will concentrate only on signal intensities.

When the average Hamiltonian, Eq. (1), is applied to a spin pair occupying a state of LM, $\rho_0 \propto \boldsymbol{I}_Z^{(i)} + \boldsymbol{I}_Z^{(j)}$, the spin system starts to oscillate between the initial state, ρ_0, and a DQ coherence, $\boldsymbol{T}_{2,+2}^{(ij)} - \boldsymbol{T}_{2,-2}^{(ij)}$, as a function of the excitation time, t_{exc}, with the frequency of the oscillation being

determined by the factor $\omega_D^{(ij)}$ and, hence, implicitly by the dipolar coupling D_{ij}:

$$\rho_0 \overset{H_{DQ}}{\rightarrow} \rho(t_{exc}) \propto \left(I_Z^{(i)} + I_Z^{(j)}\right) \cos \omega_D^{(ij)} t_{exc} + i\left(T_{2,+2}^{(ij)} - T_{2,-2}^{(ij)}\right) \sin \omega_D^{(ij)} t_{exc}. \quad (2)$$

The action of the DQ excitation can be followed by observing either the 'build-up' of the DQ coherence or the 'decay' of the LM, resulting in curves of the form

$$I_{DQ} \propto \langle \sin^2 \omega_D^{(ij)} t_{exc} \rangle \quad (3a)$$

or

$$I_{LM} \propto \langle \cos^2 \omega_D^{(ij)} t_{exc} \rangle, \quad (3b)$$

respectively. Since the observation of MQ coherences in general requires the MQ excitation to be followed by a time-reversed reconversion period [29], the DQ and LM signal intensities, I_{DQ} and I_{LM}, exhibit a squared dependence on the sine and cosine modulation, over which an additional orientational averaging procedure needs to be performed for powdered samples, as indicated by the brackets $\langle \cdots \rangle$ in the above equations. From the oscillation of such curves, the strength of the underlying dipolar pair coupling can be determined. Theoretically, the information content of I_{DQ} and I_{LM} is identical, but they differ in the state through which the system passes between excitation and reconversion. Due to its quantum order, a DQ coherence, $T_{2,+2}^{(ij)} - T_{2,-2}^{(ij)}$, is twice as sensitive to internal interactions as single-quantum coherences, and evolves under chemical shifts and homo-and heteronuclear dipolar couplings, except for the mediating coupling D_{ij}. Consequently, by introducing a spectral MQ dimension between excitation and reconversion, a two-dimensional MQ spectrum can be recorded [30]. A state of LM, on the contrary, is insensitive to all internal interactions and is only subject to spin-lattice relaxation. From an experimental point of view, this implies that DQ coherences should be particularly sensitive to experimental imperfections, while LM represents a self-contained and therefore relatively stable state. In contrast to the DQ-filtered signal however, the experimental LM signal may be contaminated by background signal from single spins which are not part of a dipolar coupled pair.

For multiple-spin systems, the evolution under the DQ Hamiltonian, Eq. (1), can no longer be described by a simple oscillation between two distinct DQ and LM states, Eq. (2), but rather by a series expansion of the form

$$\rho_0 \overset{H_{DQ}}{\rightarrow} \rho(t_{exc}) \propto I_Z - \frac{it}{1!}[H_{DQ}, I_Z] + \frac{(it)^2}{2!}[H_{DQ}, [H_{DQ}, I_Z]] \pm \ldots, \quad (4)$$

where the zeroth- and first-order terms can be identified with the familiar expressions for LM and DQ coherences,

$$I_Z = \sum_i I_Z^{(i)} \quad (5a)$$

and

$$[H_{DQ}, I_Z] = \left[\sum_{i<j} \omega_D^{(ij)} \left(T_{2,+2}^{(ij)} + T_{2,-2}^{(ij)}\right), \sum_i I_Z^{(i)}\right] = \sum_{i<j} 2\omega_D^{(ij)} \left(T_{2,+2}^{(ij)} - T_{2,-2}^{(ij)}\right), \quad (5b)$$

respectively. Using the commutator formalism and recalling the relation $[T_{l,m}^{(ij)}, I_Z^{(i)} + I_Z^{(j)}] = -m\, T_{l,m}^{(ij)}$, it can be easily shown that under the action of the DQ Hamiltonian given in Eq. (1), an initial state $\rho_0 \propto I_Z^{(i)} + I_Z^{(j)}$ evolves into a DQ coherence, $T_{2,+2}^{(ij)} - T_{2,-2}^{(ij)}$ (see Eq. (5b)), whereas inverting the sign of one of the two spins in the initial state prevents any evolution:

$$\left[H_{DQ}, I_Z^{(i)} - I_Z^{(j)}\right] = \left[\omega_D^{(ij)} \left(T_{2,+2}^{(ij)} + T_{2,-2}^{(ij)}\right), I_Z^{(i)} - I_Z^{(j)}\right] = 0. \quad (6)$$

Considering an N-spin system, in which all spins can be spectrally resolved due to their different chemical shifts, the DQ excitation can be performed independently on two subsets (N_0 and N_{inv}) of the N spins by selectively inverting the initial LM of the N_{inv} spins, while keeping the N_0 spins unaltered. In this way, DQ coherences are excited among the N_0 spins as well as among the N_{inv} spins, but no DQ coherences involve one N_{inv} spin and one N_0 spin. However, this 'decoupling' of the two subsets is limited to the evolution up to the first order in the series expansion, because only the

initial evolution can be prevented by a selective sign inversion in the initial state. Once a DQ coherence is excited, it evolves under any dipolar interaction to a third spin as follows:

$$\left[\omega_{\mathrm{D}}^{(ik)}\left(\boldsymbol{T}_{2,+2}^{(ik)}+\boldsymbol{T}_{2,-2}^{(ik)}\right),\omega_{\mathrm{D}}^{(ij)}\left(\boldsymbol{T}_{2,+2}^{(ij)}-\boldsymbol{T}_{2,-2}^{(ij)}\right)\right] = -\omega_{\mathrm{D}}^{(ik)}\,\omega_{\mathrm{D}}^{(ij)}\,\boldsymbol{I}_{\mathrm{Z}}^{(i)}\left(\boldsymbol{I}_{+}^{(j)}\boldsymbol{I}_{-}^{(k)}+\boldsymbol{I}_{-}^{(j)}\boldsymbol{I}_{+}^{(k)}\right). \quad (7)$$

This commutator is part of the second-order term in the series expansion, Eq. (4). The first term in the commutator reflects the average Hamiltonian of the DQ pulse sequence with respect to the spins i and k, while the second term represents a (selected) DQ coherence between the spins i and j. The commutator does not vanish, indicating an evolution of the (ij)-DQ coherence into a three-spin zero-quantum state, whose contribution relative to the (ij)-DQ coherence is initially weighted by the factor $\omega_{\mathrm{D}}^{(ik)}$ and, hence, by the strength of the perturbing coupling D_{ik}. Consequently, the regime of two 'decoupled' subsets persists up to a time which is determined by the strength of the perturbing coupling. From an experimental point of view, it should be noted that a zero-quantum state cannot be distinguished from LM, if only RF phase cycling is applied for coherence selection.

Considering this evolution into a higher-spin state, the major difference between a spin-selective recoupling method, such as RR, and the SIMQEX approach presented here becomes obvious. In the RR method, the dipolar interactions between two specific types of spins are selectively recoupled, while all other interactions are removed by MAS. On the contrary, for SIMQEX, the modification of the initial state prevents only the initial dipolar evolution, but it does not affect the dipolar recoupling performance, since the pulse sequence applied for DQ excitation continuously recouples *all* dipolar interactions. As a consequence of this interplay, the evolution of a selectively inverted initial state can be separated into two regimes: firstly, the initial DQ excitation for short excitation times, and secondly the DQ evolution for longer excitation times. During the first, the spin system is effectively separated into two subsets, and the generation of DQ coherences between the two subsets is suppressed, while during the latter, the DQ coherences of one subset start to evolve also under the dipolar interactions to the other subset. This evolution reflects the dipolar couplings and, hence, the geometry of the entire spin system, while the initial excitation provides individual access to the geometry of the two subsystems.

3. Experiments

The experiments were performed on a Bruker DSX spectrometer operating at ^{1}H and ^{13}C Larmor frequencies of 400 and 100 MHz, respectively. A double resonance MAS probe supporting rotors of 7 mm outer diameter was used, allowing maximum ^{1}H RF fields of $\omega_{1,\mathrm{H}}/2\pi \approx 100$ kHz for ^{1}H decoupling. The MAS frequency was set to $\omega_{\mathrm{R}}/2\pi = 5$ kHz. The pulse sequence for the LM- and DQ-filtered experiments is schematically depicted in Fig. 1a. After a Hartmann–Hahn cross-polarisation (CP) from ^{1}H to ^{13}C with a contact time of 1 ms, applying an amplitude ramp from 60% to 100% on the ^{13}C contact pulse, the ^{13}C polarisation is transferred into a longitudinal state by a $\pi/2$-pulse. To invert the longitudinal polarisation of a selected type of spins, a DANTE π-pulse is applied [31]. The DANTE pulse consisted of 40 pulses of 0.5 μs duration, which were separated by free-precession intervals of 20 μs duration.

After preparing the initial state, ^{13}C–^{13}C DQ coherences were excited and reconverted using the C7 recoupling pulse-sequence [5], with the excitation time ranging between 0 and 2.4 ms. To minimise off-resonance effects on the DQ excitation efficiency, the ^{13}C transmitter frequency was set at, or close to, the centre of the nuclear resonance frequencies of the spins to be excited. The coherence transfer pathway was directed either through a DQ coherence or through a LM state between excitation and reconversion, as depicted in Fig. 1b. The overall phase cycle consisted of 64 steps. For ^{1}H decoupling, a continuous ^{1}H RF field was applied at $\omega_{1,\mathrm{H}}/2\pi \approx 100$ kHz during the DANTE and the C7 pulse trains, while a TPPM scheme [32] with a phase flip angle of 15° was used at $\omega_{1,\mathrm{H}}/2\pi \approx 70$ kHz during the signal detection.

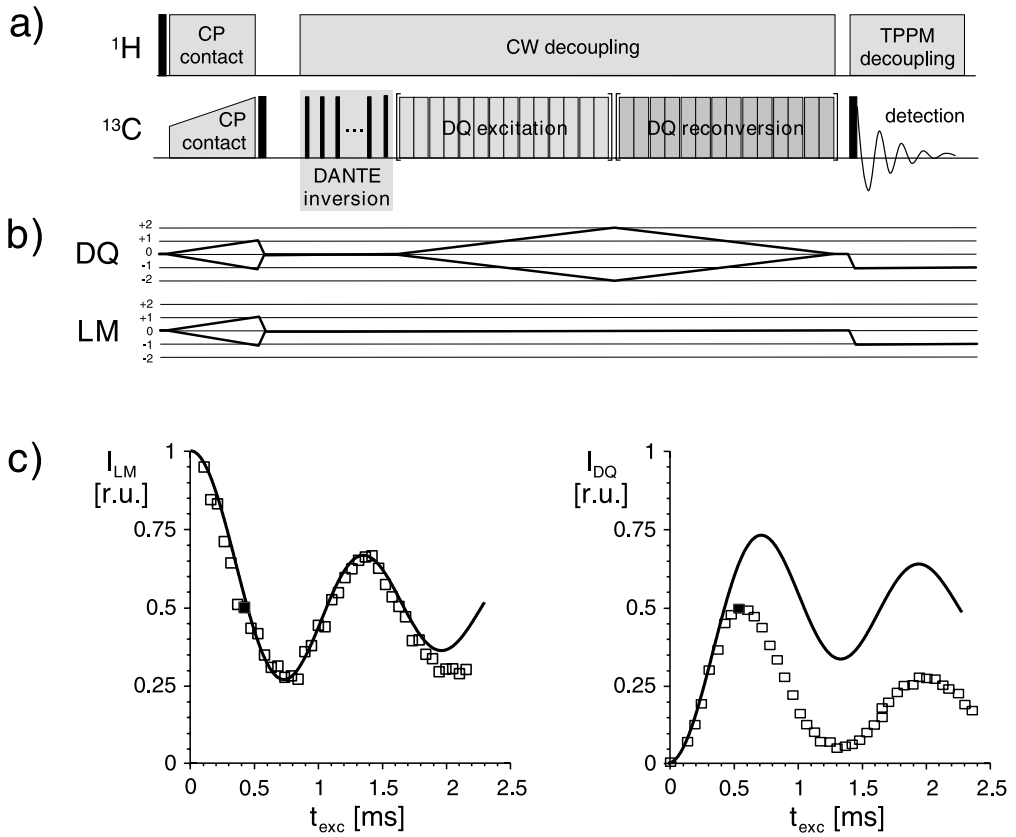

Fig. 1. (a) Schematic representation of the pulse sequence applied for DQ- and LM-filtered experiments. The selective inversion of spins is achieved by a DANTE π-pulse, and DQ coherences are excited and reconverted by a C7 pulse sequence. (b) Coherence transfer pathway for the DQ- and LM-filtered versions of the experiment, as selected by an appropriate phase cycle. (c) LM decay and DQ build-up curves. The theoretical spin pair curves (solid lines) are compared to experimental data recorded on the ^{13}C spin pair in $^{13}C_2$-glycine (squares). The filled squares indicate the data points, for which the intensity calibration $I_{LM} + I_{DQ} = 1$ has been performed.

The samples investigated were approximately 5 mg of uniformly ^{13}C-labelled glycine and L-alanine, which were diluted by recrystallisation from methanol with the respective unlabelled material in a 1:10 ratio. The signal intensities detected in the LM- and DQ-filtered experiments, I_{LM} and I_{DQ}, were calibrated using the spectra obtained for $t_{exc} = 2\tau_R = 400$ μs by setting $I_{LM} + I_{DQ} = 1$. For the LM decay curves, a small constant value was subtracted from all data points in order to correct for the background signal from isolated nuclei in natural abundance. In addition, the first two experimental data points (i.e., for $t_{exc} = 0$ μs and $t_{exc} = 57.14$ μs) were ignored due to a significant deviation from the curves. In general, the background signal in LM experiments can be excluded by referencing to the oscillating part of the LM decay curve.

4. Results and discussion

As a starting point, the LM- and DQ-filtered experiments were performed on an initial state of LM without any selective inversion by omitting the DANTE pulse in Fig. 1a. The LM decay and the DQ build-up curves obtained for the ^{13}C spin pairs in $^{13}C_2$-labelled glycine are displayed in Figs. 1c (squares) and compared to the theoretical curves (solid lines) according to Eqs. (3a) and (3b)

for a spin pair with a dipolar coupling of $D_{ij}/2\pi = 2.2$ kHz, corresponding to a ^{13}C–^{13}C internuclear distance of 0.151 nm. Both experimental curves show the characteristic initial increase up to $t_{exc} \approx 0.5$ ms, corresponding to $D_{ij}t_{exc}/2\pi \approx 1$, followed by an oscillation whose frequency agrees with the behaviour expected from Eqs. (3a) and (3b). However, while the LM-decay curve accurately resembles the theoretical curve up to $t_{exc} < 2$ ms, the DQ build-up is already strongly affected by relaxation for short excitation times ($t_{exc} > 0.5$ ms). This deviation indicates that even for a spin pair model compound, the DQ-filtered version of the experiment suffers more from experimental imperfections, such as insufficient heteronuclear decoupling, RF field inhomogeneities and pulse imperfections, than the LM-filtered version. At first sight, this corresponds to the pronounced sensitivity of DQ coherences to perturbing interactions, while LM states are largely

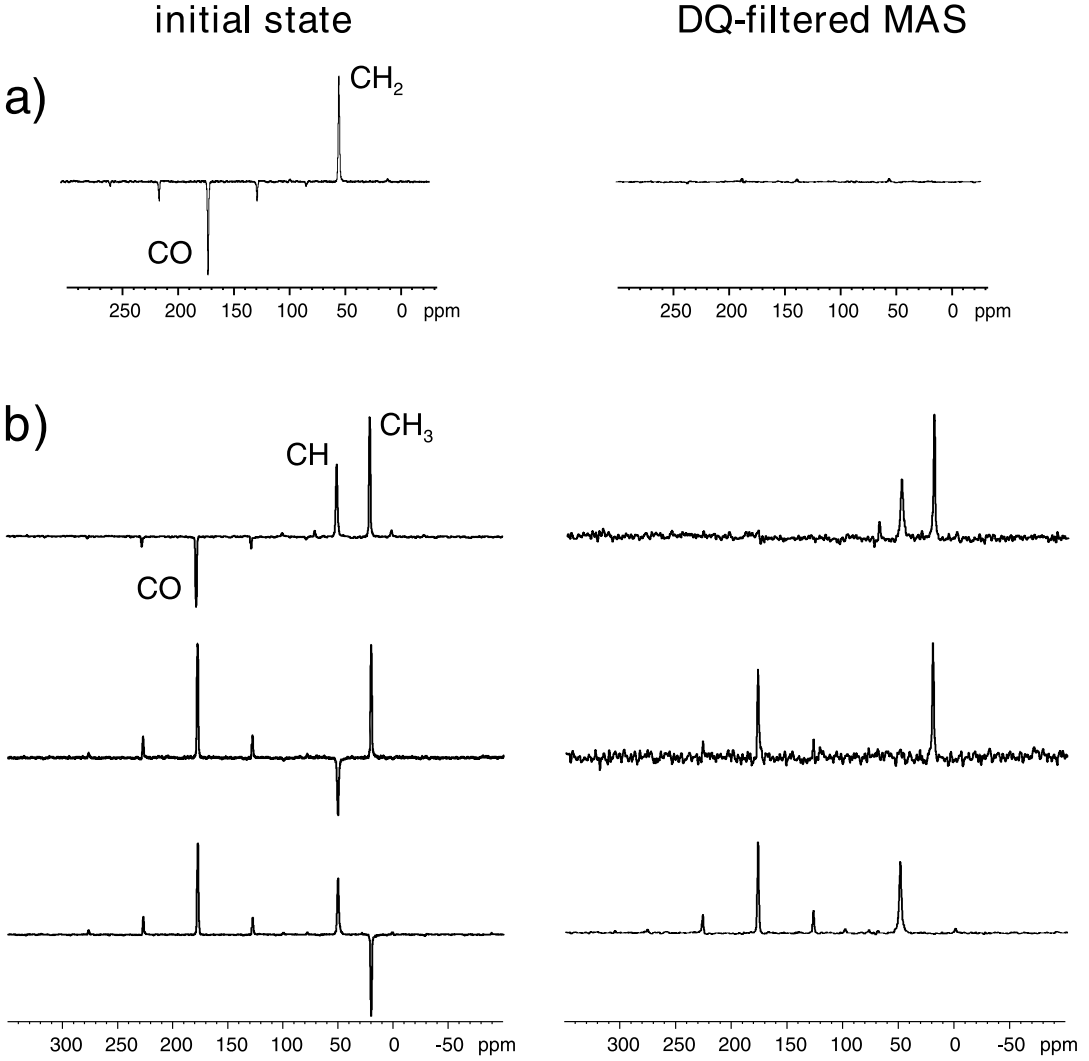

Fig. 2. ^{13}C CP MAS and DQ-filtered MAS spectra of: (a) $^{13}C_2$-glycine and (b) $^{13}C_3$-alanine. On the left, the initial states are shown, out of which the DQ-filtered spectra on the right are generated by applying a C7 pulse train for $t_{exc} = 800$ μs.

insensitive. A closer inspection reveals that the two versions of the experiment differ, firstly, in the state whose properties are used for coherence selection by phase cycling and, secondly, in the state which predominates for short excitation times. For longer excitation times ($D_{ij}\,t_{exc} > 1$), the two-spin system oscillates between the LM and DQ state, such that both contribute equally. Consequently, the observed differences (Fig. 1c) could be due to coherence losses in the course of the experimental DQ selection, or due to different relaxation behaviour of DQ and LM states during the initial periods of the curves. In addition, it should be noted that the LM decay data is corrected for contributions of background signal by subtracting a constant offset value. Although some relaxation effects may be concealed in the LM decay curve as a result of this correction procedure, it cannot serve as an explanation for the obvious differences observed in the oscillations of both curves.

The effect of including a preceding selective inversion pulse on the DQ excitation efficiency is shown for ^{13}C spectra of $^{13}C_2$-glycine and $^{13}C_3$-alanine in Figs. 2a and 2b, respectively. The CP MAS spectra on the left reflect the initial states generated by applying a DANTE inversion pulse selectively to one of the spins, and the DQ-filtered spectra on the right represent the DQ coherences excited by applying a C7 pulse train for $t_{exc} = 0.8$ ms. For the ^{13}C spin pair in glycine, the inversion of one of the spins prevents DQ excitation, while for the ^{13}C three-spin system in alanine a pair of spins can be selectively excited by inverting the third spin. In this way, each of the two strongly coupled ^{13}C pairs, CO–CH and CH–CH_3, can be effectively decoupled from the CH_3 and the CO spin, and even the DQ coherence of the weakly coupled $CO\cdots CH_3$ pair can be selectively excited without any contribution from the stronger CO–CH and CH–CH_3 coherences, as proved by the absence of CH signal. The latter observation, in particular, provides clear evidence for the decoupling performance achievable by SIMQEX.

The decoupling effect is expected to vanish gradually for long DQ excitation times (see above), because it is not based on a selective recoupling technique, but rather on a selective excitation of DQ coherences, which are subject to all (recoupled) dipolar interactions in the spin system, once they are excited. It is therefore interesting to explore how long the DQ coherences remain unaffected when increasing the excitation time, and to what extent LM decay or DQ build-up curves can be used to individually measure a spin pair coupling in the presence of perturbing couplings.

In Fig. 3, the results of numerical simulations of two-spin and linear three-spin ^{13}C systems with internuclear distances of 0.156 nm and 0.312 nm are displayed. The arrangement of the spins is schematically depicted above the diagrams, where the nuclei, from which signal is detected, are shaded. In Fig. 3a, a strongly coupled pair with a distance of 0.156 nm, corresponding to a dipolar coupling of $D_{ij}/2\pi = 2.0$ kHz, is considered in the isolated case (pair), and in the presence of a third spin which perturbs the pair by a coupling of $D_{jk}/2\pi = 2.0$ kHz to one of the pair spins, and whose polarisation is oriented either parallel (3s) or anti-parallel (inv) with respect to the pair. In Fig. 3b, the same cases are considered (pair/3s/inv), but the perturbing spin is now located in the centre of a weakly coupled pair, such that a pair with a distance of 0.312 nm, corresponding to a dipolar coupling of $D_{ij}/2\pi = 0.25$ kHz, is strongly perturbed by two dipolar couplings of $D_{jk}/2\pi =$ 2.0 kHz to the third spin.

For the isolated pair, the LM decay and the DQ build-up curves (dotted lines) show the familiar initial decrease and increase, respectively, which is, in the case of the strongly coupled pair (Fig. 3a), followed by oscillations (see Fig. 1c for comparison). In the three-spin case without inversion (dashed lines), the LM decay is initially dominated by the strong dipolar couplings, before it enters a regime of complicated and superimposed oscillations. The corresponding DQ build-up curves show a very short initial increase, before a well defined oscillation sets in, whose frequency is higher than expected from Eq. (3a) for the strong coupling. Thus, these curves cannot be used to determine the dipolar coupling strengths in the spin systems due to the perturbations caused by the additional spin, whose destructive influence is most drastically observed for the case of a weak coupling which is subject to a strong perturbation (Fig. 3b). However, when the perturbing spin is

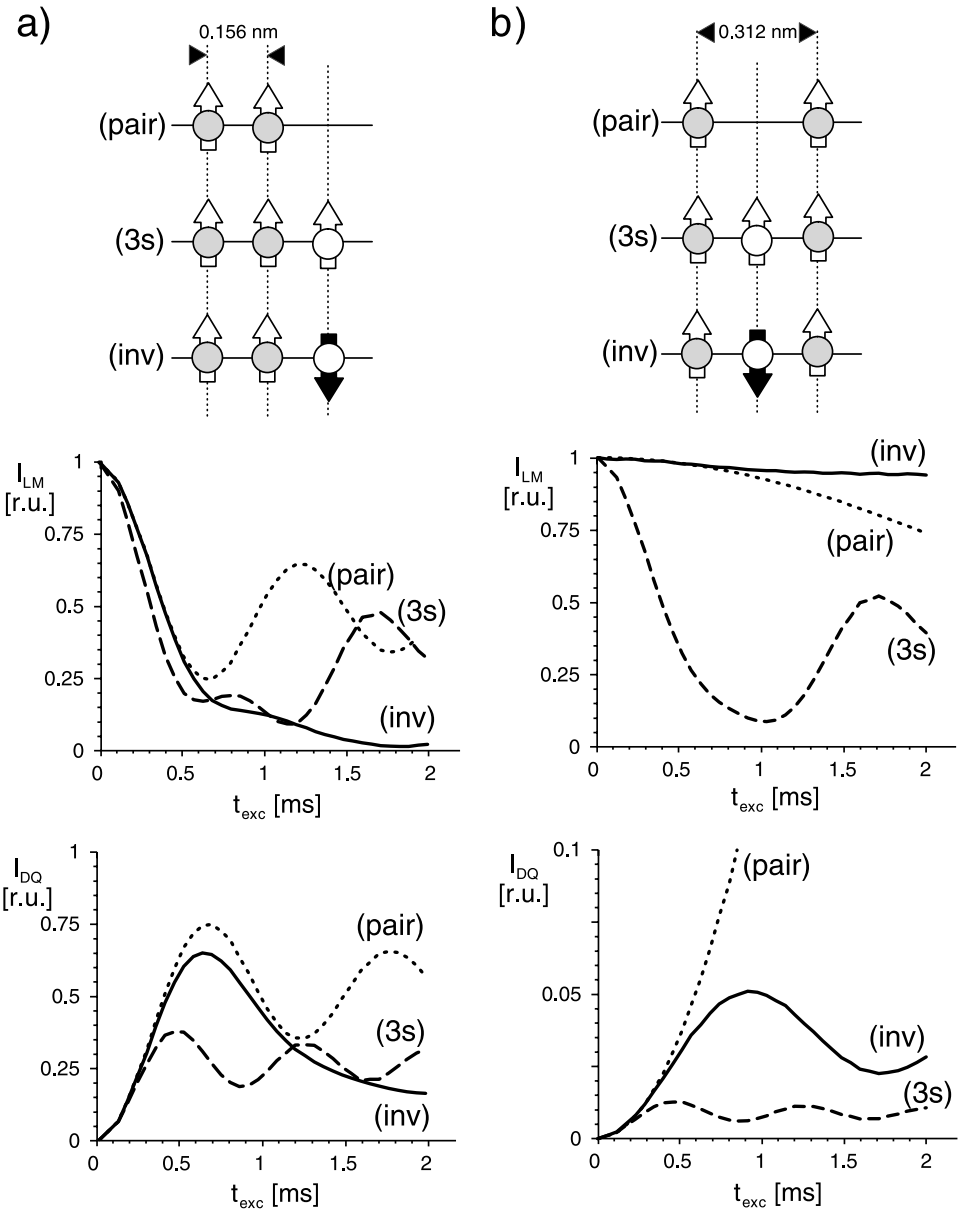

Fig. 3. Numerical simulations of LM decay and DQ build-up curves for two-spin and linear three-spin systems. A pair of ^{13}C spins with an internuclear distance of: (a) 0.156 nm and (b) 0.312 nm is considered (as indicated by the grey shading of the atoms), and the effect of the dipolar interactions to a third spin with and without selective inversion is simulated.

selectively inverted, the calculated curves (solid lines) resemble the initial behaviour of the respective pair up to about $t_{exc} \approx 0.5$ ms and can, in this limit, be used as a reasonable approximation for the two-spin case. As has been derived from Eq. (7), the initial period of the excitation time, $t_{exc} < t_{max}$, is limited by the strongest couplings D_{max} present in the system and, considering the simulations, the limit can be estimated according to $D_{max} t_{max}/2\pi \approx 1$. The initial decoupling effect

even allows the weakly coupled pair to be investigated selectively under a strong perturbation by a central spin, while without the inversion the signal of the weakly coupled pair is completely concealed by the strong interactions.

After considering a linear three-spin system in the simulations, we now turn to SIMQEX experiments performed on the ^{13}C three-spin system in alanine. Fig. 4 shows the LM decay and the DQ build-up curves recorded for the 'unaltered' spin system (left) and after inverting the CO (middle) and the CH_3 spin (right). For the 'unaltered' spin system, no clear oscillations are visible in the LM decay or the DQ build-up. In the LM decay, the central CH spin can be identified by its faster decay rate, while for the DQ build-up the pronounced relaxation does not allow any specific information to be obtained from the curves. Inverting the CO and the CH_3 spin significantly reduces the perturbation of the strongly coupled CH–CH_3 and CO–CH pair, respectively, such that the oscillations clearly appear in the curves, allowing the coupling strengths of the pairs to be determined individually. The value obtained from the curves is $D_{ij}/2\pi = (2.1 \pm 0.1)$ kHz, corresponding to a distance of (0.153 ± 0.003) nm. As observed for the two-spin system in glycine (Fig. 1c), the DQ build-up is far more strongly affected by relaxation than the LM decay.

Figs. 5a and 5b show the SIMQEX results obtained for the weakly coupled CO$\cdots$$CH_3$ pair after inverting the central CH spin. In comparison to the curves obtained for the 'unaltered' three-spin system (Fig. 4, left), it is clear that inverting

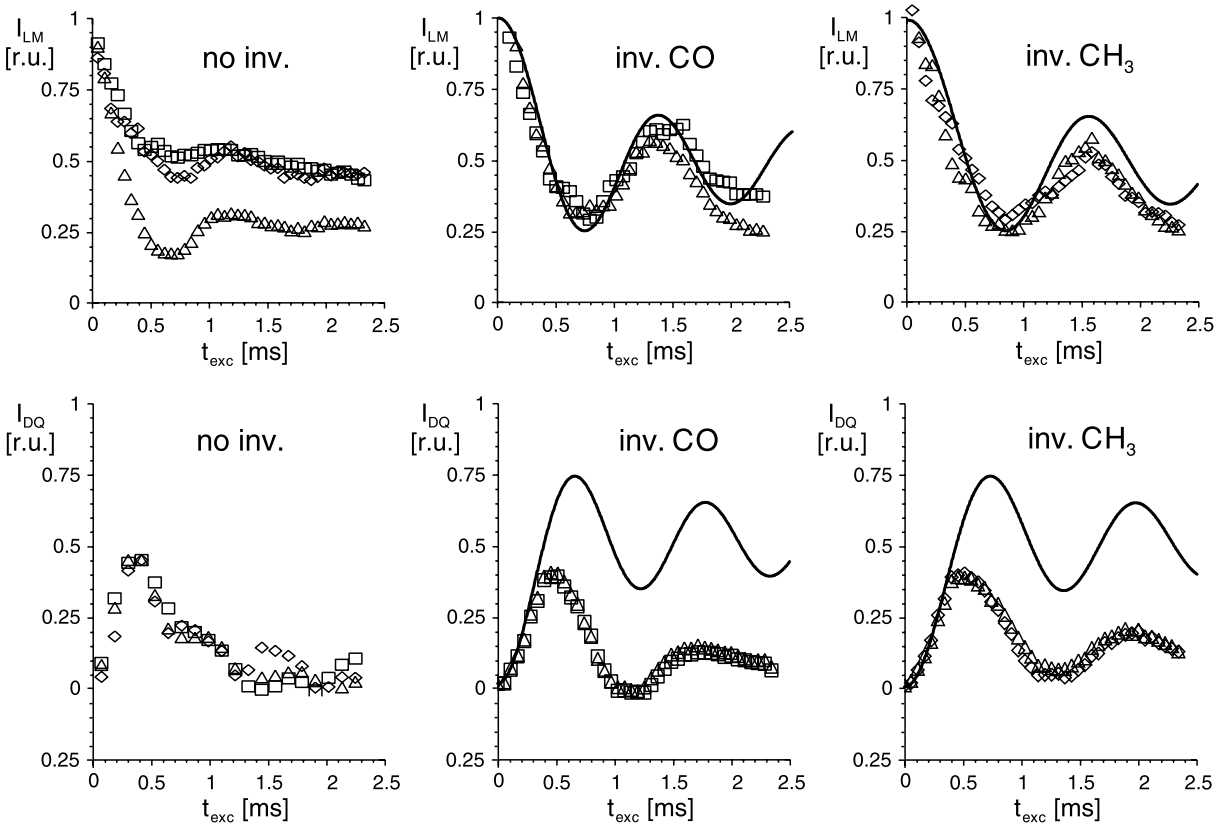

Fig. 4. LM decay and DQ build-up curves for $^{13}C_3$-alanine without inversion (left), after inverting the ^{13}CO spin (middle) and after inverting the $^{13}CH_3$ spin (right). The experimental data points ($^{13}CH_3$: squares, ^{13}CH: triangles, ^{13}CO: diamonds) are compared to theoretical spin pair curves (solid lines) for $D_{ij}/2\pi = (2.1 \pm 0.1)$ kHz.

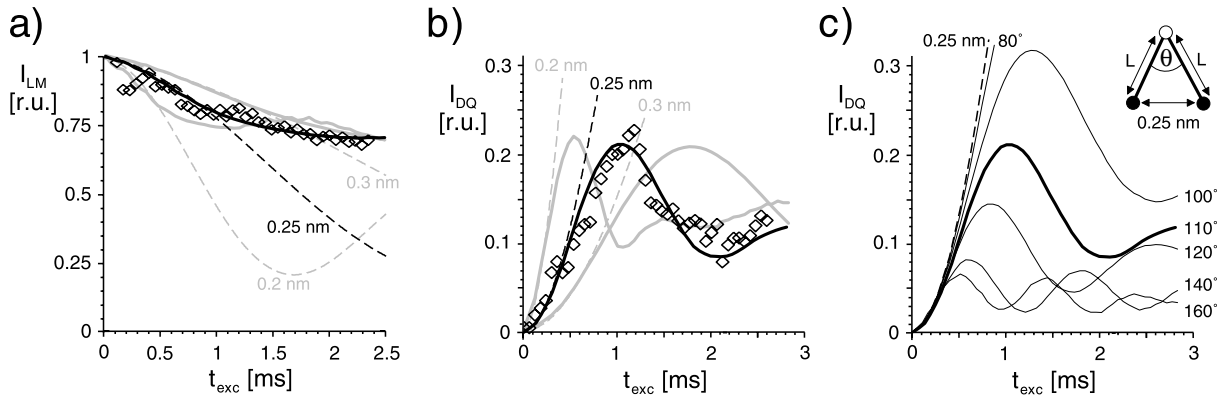

Fig. 5. (a) LM decay and (b) DQ build-up curve recorded for the ^{13}CO spin in $^{13}C_3$-alanine after inverting the ^{13}CH spin (identical curves are obtained for the $^{13}CH_3$-spin). The experimental data are compared to theoretical spin pair curves (dashed lines) and simulated curves which take into account the entire three-spin geometry in alanine (solid lines). For the LM decay, a slight exponential decay with a time constant of 16 ms is included in the calculations. The black curves represent the alanine structure with a pair distance of 0.25 nm, while the grey curves with pair distances of 0.20 and 0.30 nm allow the accuracy of the determination to be estimated to approx. ±0.02 nm. (c) Simulated DQ build-up curves for planar three-spin systems, as depicted in the inset. The perturbing spin (white) is inverted and the DQ coherence of the other two spins (black) with an internuclear distance of 0.25 nm is considered. The angle θ is varied between 20° and 180°, corresponding to a variation of the 'bond length', L, between 0.720 and 0.125 nm.

the CH spin leads the LM to decay much more slowly (Fig. 5a), and the initial behaviour resembles the decay expected for a pair with an internuclear distance of 0.25 nm (dashed line), in accordance with the structure of alanine [33]. The same observations apply accordingly for the DQ build-up curves (Fig. 5b), where the initial increase agrees with the respective pair curve (dashed line), while for longer excitation times an oscillation sets in, reflecting the geometry of the three-spin system and the presence of perturbing couplings. The solid curves, which match the experimental data very accurately for both the LM decay (Fig. 5a) and the DQ build-up curves (Fig. 5b), result from exact numerical simulations of the ^{13}C three-spin system in alanine with C–C bond lengths of 0.152 nm and a C–C–C angle of 110° (see the calculated curves in Fig. 3 for comparison). The accuracy of the long distance determination (0.25 nm) can be estimated by comparing the experimental data with the grey curves in the diagrams, which represent spin pairs with distances of 0.20 and 0.30 nm.

The simulated DQ build-up curves in Fig. 5c demonstrate how the spin-system geometry affects the long-time behaviour of the curves through perturbing dipolar interactions. In analogy to Fig. 5b, the $CO\cdots CH_3$ pair in alanine is considered and its internuclear distance is kept at 0.25 nm, while the CH spin is displaced such that the C–C–C angle, θ, ranges from 20° to 180°, corresponding to varying the C–C 'bond lengths', L, between 0.720 and 0.125 nm (as indicated by the inset in Fig. 5c). Small C–C–C angles correspond to long CO–CH and CH–CH_3 distances and, consequently, to weak perturbations of the $CO\cdots CH_3$ DQ coherence, such that the DQ build-up curve shows spin pair behaviour. Perturbing effects become clearly visible in the form of increasing oscillation frequencies for $\theta > 80°$, corresponding to $L < 0.20$ nm, which means that each of the two perturbing couplings is more than twice as strong as the CO–CH_3 coupling. For $80° < \theta < 180°$, the long-time behaviour, $0.5\ \text{ms} < t_{exc} < 3\ \text{ms}$, is very sensitive to the perturbations, allowing the precise determination of the three-spin geometry, while in the initial regime, $t_{exc} < 0.5$ ms, the curves still coincide with the 0.25 nm spin pair behaviour, allowing the separate determination of the $CO\cdots CH_3$ distance.

5. Conclusions

Selective inversion of spins before applying dipolar recoupling pulse-sequences provides a high degree of mutual homonuclear decoupling between spins of opposite polarisation in the initial period of DQ excitation. In this way, DQ coherences can be selectively excited for distinct spin pairs and, moreover, dipolar coupling strengths can be individually determined in the presence of perturbing couplings, even for weakly coupled spin pairs which are subject to other strong couplings. In this respect, the SIMQEX approach is complementary to RR techniques, because the selectivity achievable by inversion does not rely on a specific choice of the MAS frequency, and can be readily combined with any of the dipolar recoupling techniques available for MQ excitation. In addition, selective inversion can be accomplished by various methods and can be executed on different combinations of spins of the system under investigation.

As an explanatory example, consider a five ^{13}C-spin system of the form C_1–C_2–C_3–O–C_4–C_5 with five resolved ^{13}C resonances. As a starting information, the connectivities of the carbons and the assignment of the resonance lines are readily available from two-dimensional ^{13}C–^{13}C MAS spectra by means of through-bond correlation spectroscopy [34] or dipolar DQ spectroscopy [10,35]. Using SIMQEX and focusing on the *initial* behaviour of the LM decay or DQ build-up curves, the ^{13}C–^{13}C dipolar couplings, D_{ij}, can then be individually measured for the pairs $C_i \cdots C_j$ by inverting the spins i and j out of the five resonance lines. In addition to the bond lengths, the two-bond distances $C_1 \cdots C_3$ and $C_3 \cdots C_4$ and, hence, the bond angles C_1–C_2–C_3 and C_3–O–C_4 are obtainable in direct analogy to the alanine case. The three-bond ^{13}C–^{13}C distances $C_2 \cdots C_4$ and $C_3 \cdots C_5$ provide access to the respective torsion angles. Although, depending on the molecular geometry, the latter dipolar couplings may be relatively weak, the SIMQEX LM decay or DQ build-up curves still contain pair-specific information in the limit of short excitation times, because the limit depends on the strength of the perturbing couplings rather than on the strength of the selected coupling. At this point, the geometry of the five-spin system is, at a first instance, completely probed, and the data can then serve as a starting model for numerical simulations of, e.g., the long-time behaviour of the LM decay or DQ build-up curves, allowing a further refinement of the geometrical parameters.

In general, SIMQEX opens up a variety of new possibilities for dipolar MQ MAS experiments which can be performed on multiple-spin systems, as they are encountered in samples containing multiple labels or labelled molecular fragments, provided that the resonance lines of interest are sufficiently resolved. Moreover, the approach can also be readily implemented in two-dimensional MQ MAS spectroscopy and in MQ experiments exploiting MAS sideband patterns for the determination of dipolar couplings.

Acknowledgements

I.S. is indebted to Karena Thieme (MPI for polymer research, Mainz, Germany) for inspiring discussions, and thanks the Deutsche Forschungsgemeinschaft for a Research Fellowship. A.W. thanks the BBSRC for a Senior Fellowship. Financial support from BBSRC (43/B04750) and HEFCE is gratefully acknowledged.

References

[1] A.E. Bennett, R.G. Griffin, S. Vega, in: P. Diehl, E. Fluck, H. Günter, R. Kosfeld, J. Seelig (Eds.), NMR Basic Principles and Progress, vol. 33, Springer, Berlin, 1994, pp. 1–77.
[2] B.H. Meier, W.L. Earl, J. Chem. Phys. 85 (1986) 4905.
[3] R. Tycko, G. Dabbagh, J. Am. Chem. Soc. 113 (1991) 9444.
[4] N.C. Nielsen, H. Bildsoe, H.J. Jakobsen, M.H. Levitt, J. Chem. Phys. 101 (1994) 1805.
[5] Y.K. Lee, N.D. Kurur, M. Helmle, O.G. Johannessen, N.C. Nielsen, M.H. Levitt, Chem. Phys. Lett. 242 (1995) 304.
[6] M. Feike, D.E. Demco, R. Graf, J. Gottwald, S. Hafner, H.W. Spiess, J. Magn. Reson. A 122 (1996) 214.
[7] M. Hohwy, H.J. Jakobsen, M. Edén, M.H. Levitt, N.C. Nielsen, J. Chem. Phys. 108 (1998) 2686.
[8] C.M. Rienstra, M.E. Hatcher, L.J. Mueller, B. Sun, S.W. Fesik, R.G. Griffin, J. Am. Chem. Soc. 120 (1998) 10602.

[9] M. Hohwy, C.M. Rienstra, C.P. Jaroniec, R.G. Griffin, J. Chem. Phys. 110 (1999) 7983.
[10] A. Brinkmann, M. Edén, M.H. Levitt, J. Chem. Phys. 112 (2000) 8539.
[11] D.M. Gregory, M.A. Metha, J.C. Shiels, G.P. Drobny, J. Chem. Phys. 107 (1997) 28.
[12] F. Creuzet, A. McDermott, R. Gebhardt, K. van der Hoef, M.B. Spijker-Assink, J. Herzfeld, J. Lugtenburg, M.H. Levitt, R.G. Griffin, Science 251 (1991) 783.
[13] O.B. Peersen, S. Yoshimura, H. Hojo, S. Aimoto, S.O. Smith, J. Am. Chem. Soc. 114 (1992) 4332.
[14] A.E. McDermott, F. Creuzet, R. Gebhard, M. van der Hoef, H.J. Lewitt, J. Herzfeld, J. Lugtenburg, R.G. Griffin, Biochemistry 33 (1994) 6129.
[15] P.J.E. Verdegem, M. Helmle, J. Lugtenburg, H.J.M. deGroot, J. Am. Chem. Soc. 119 (1997) 169.
[16] X. Feng, P.J.E. Verdegem, Y.K. Lee, M. Helmle, S.C. Shekar, H.J.M. deGroot, J. Lugtenburg, M.H. Levitt, Sol. State NMR 14 (1999) 81.
[17] K. Nomura, K. Takegoshi, T. Terao, K. Uchida, M. Kainosho, J. Am. Chem. Soc. 121 (1999) 4064.
[18] K. Schmidt-Rohr, J. Am. Chem. Soc. 118 (1996) 7601.
[19] X. Feng, M. Eden, A. Brinkmann, H. Luthman, L. Eriksson, A. Graslund, O.N. Antzutkin, M.H. Levitt, J. Am. Chem. Soc. 119 (1997) 12006.
[20] X. Feng, P.J.E. Verdegem, D. Sandstrom, Y.K. Lee, M. Edén, B.H.M. BoveeGeurts, W.J. deGrip, J. Lugtenburg, H.J.M. deGroot, M.H. Levitt, J. Am. Chem. Soc. 119 (1997) 12006.
[21] M. Hong, W. Hu, J.D. Gross, R.G. Griffin, J. Magn. Reson. 135 (1998) 169.
[22] X. Feng, P.J.E. Verdegem, M. Eden, D. Sandstrom, Y.K. Lee, B.H.M. BoveeGeurts, W.J. deGrip, J. Lugtenburg, H.J.M. deGroot, M.H. Levitt, J. Biomol. NMR 16 (2000) 1.
[23] M. Edén, A. Brinkmann, H. Luthman, L. Eriksson, M.H. Levitt, J. Magn. Reson. 144 (2000) 266.
[24] D.P. Raleigh, M.H. Levitt, R.G. Griffin, Chem. Phys. Lett. 146 (1988) 71.
[25] M.H. Levitt, D.P. Raleigh, F. Creuzet, R.G. Griffin, J. Chem. Phys. 92 (1990) 6347.
[26] N.C. Nielsen, F. Creuzet, R.G. Griffin, M.H. Levitt, J. Chem. Phys. 96 (1992) 5668.
[27] T. Karlsson, M. Eden, H. Luthman, M.H. Levitt, J. Magn. Reson. 145 (2000) 95.
[28] T. Karlsson, M.H. Levitt, submitted.
[29] M. Munowitz, A. Pines, Adv. Chem. Phys. 66 (1987) 1.
[30] H. Geen, J. Gottwald, R. Graf, I. Schnell, H.W. Spiess, J.J. Titman, J. Magn. Reson. 125 (1997) 224.
[31] G. Bodenhausen, R. Freeman, G.A. Morris, J. Magn. Reson. 23 (1976) 171.
[32] A.E. Bennett, C.M. Rienstra, M. Auger, K.V. Lakshmi, R.G. Griffin, J. Chem. Phys. 103 (1995) 6951.
[33] M.S. Lehmann, T.F. Koetzle, W.C. Hamilton, J. Am. Chem. Soc. 94 (1972) 2657.
[34] M. Baldus, R.J. Iuliucci, B.H. Meier, J. Am. Chem. Soc. 119 (1997) 1121.
[35] M. Hong, J. Magn. Reson. 136 (1999) 86.